1-1-1968

Feasibility of Rating Current Meters in a Velocity Field

Gaylord V. Skogerboe

Lloyd H. Austin

Roland W. Jeppson

Chi-Yuan Wei

FEASIBILITY OF RATING CURRENT METERS IN A VELOCITY FIELD

Final Report of USGS Contract
No. 14-08-0001-10867
April 1, 1967 to December 31, 1967

Submitted to

U. S. Geological Survey
Department of the Interior

Prepared by

Gaylord V. Skogerboe
Lloyd H. Austin
Roland W. Jeppson
Chi-Yuan Wei

Utah Water Research Laboratory
College of Engineering
Utah State University
Logan, Utah

January 1968 Report PR-WG51-1

ABSTRACT

FEASIBILITY OF RATING CURRENT METERS IN A VELOCITY FIELD

Preliminary studies employed an 8-inch (outlet diameter) contracting cone and an 8-inch converging nozzle. The design of the cone is based on an electromagnetic analogy reported by Smith and Wang, while the nozzle was designed assuming potential flow and using numerical methods to obtain the solution. Both designs yielded fairly uniform velocity fields, any deviations being primarily due to either construction or measurement techniques. The towing tank rating for a Pygmy current meter was compared with the submerged jet rating, the difference being 1 or 2 percent. A Prototype system was constructed using a 16-inch contracting cone (d). Two Type AA Price current meters were rated in this facility. The hydraulic performance of the system proved very satisfactory, illustrating that rating current meters in a submerged jet emanating from a contracting cone is feasible.

Skogerboe, Gaylord V., Lloyd H. Austin, Roland W. Jeppson, and Chi-Yuan Wei. FEASIBILITY OF RATING CURRENT METERS IN A VELOCITY FIELD. Final report to U. S. Geological Survey, Department of the Interior. Report WG 51-1, Utah Water Research Laboratory, College of Engineering, Utah State University, Logan, Utah. January 1968.

KEY WORDS -- *current meter current meter rating flow measurement hydraulics *open channel flow open channel flow measurement *submerged jet.

ACKNOWLEDGMENTS

The writers wish to express their gratitude and sincere appreciation to the many individuals who assisted in this research effort.

The U. S. Geological Survey (USGS) has sponsored this feasibility investigation of rating current meters in a velocity field. The possibility of rating current meters in a submerged jet was suggested by George F. Smoot, Water Resources Division, USGS. Mr. Smoot acted as technical officer during the conduct of this study and was very instrumental in its success.

The fabrication of the model cones and the prototype rating system was supervised by Mr. Kenneth Steele with Messrs. Gilbert Peterson, Verl Bindrup, Rex Condie and Keith Miller participating. The writers are indebted to the shop personnel for their efforts in meeting a strict time schedule.

Mr. Brent B. Hacking assisted with the data collection during both the model and prototype studies, while Mr. Wynn R. Walker participated in the data collection and analysis from the prototype system. The efforts of both these gentlemen in working around-the-clock in order to complete the study on schedule was very much appreciated.

Gaylord V. Skogerboe
Lloyd H. Austin
Roland W. Jeppson
Chi-Yuan Wei

INTRODUCTION

Background

Current meters presently are being calibrated in a towing tank. This technique is described by the U. S. Geological Survey (1962).

> The meter rating station operated by the National Bureau of Standards in Washington, D. C., consists of a reinforced concrete basin 400 feet long, 6 feet wide, and 6 feet deep. On the sides and extending the entire length of the basin are steel rails which carry an electric rating car. This car is operated to move the current meter at a constant rate of speed through the still water in the basin. Although the rate of speed can be accurately adjusted by means of a hydraulic regulating gear, the average velocity of the moving car is determined for each run by making an independent measurement of the distance it travels during the time that the revolutions of the bucket wheel are elctrically counted. A scale graduated to feet and tenths along the side of the basin is used for this purpose. From 8 to 10 pairs of runs are usually made in the rating of each current meter. A pair of runs generally consists of two traverses of the basin, one run in each direction, at approximately the same speed. Practical considerations usually limit the ratings to velocities ranging from one-tenth of a foot per second to about 15 feet per second, although the rating car can be operated at both higher and lower speeds. For ordinary ratings, however, neither of these extremes is used; and unless a special request is made, the lowest velocity used in the rating is about 0.2 foot per second, and the highest is about 9.0 feet per second.

Less time would be required for the ratings because once the velocity field is established, one current meter after another could be placed in the moving fluid. A current meter would be calibrated in a number of uniform velocity fields, each field having a specified magnitude. The calibration resulting from each uniform velocity field would establish the rating for the meter.

BOUNDARIES PRODUCING UNIFORM VELOCITIES

Rating current meters in a submerged jet can only be feasible if it is possible to produce a uniform velocity field. Two separate methods are available for designing boundaries which will produce a jet having a uniform velocity field. The first method employs an electromagnetic analogy to yield a family of contracting cone (Fig. 1) geometries (Smith and Wang, 1944). The second method (Jeppson 1966), utilizes recent developments in numerical methods for designing converging nozzles (Fig. 2). A brief description of each method is given below.

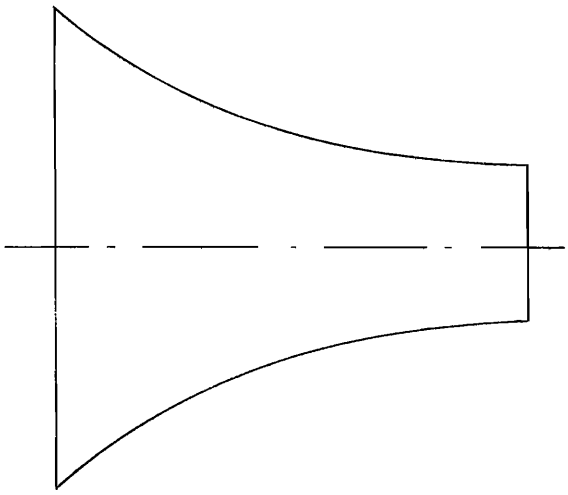

Fig. 1. Contracting cone.

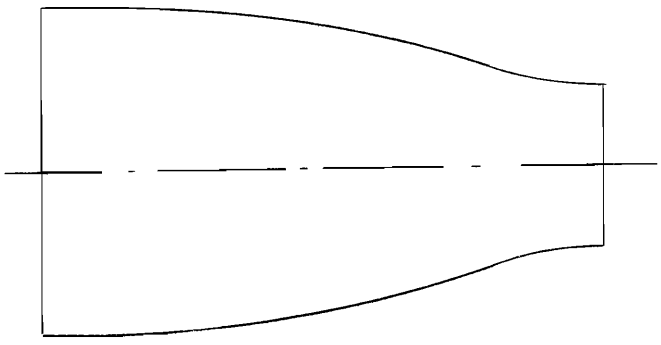

Fig. 2. Converging nozzle.

Electromagnetic Analogy

Smith and Wang (1944) have used the analogy between the magnetic field that is created by two coaxial and parallel coils carrying electrical current and the velocity field that is created by two corresponding ring vortices to develop the geometric form of contracting cones having uniform velocities at the throat. The following excerpts, including Figs. 3, 4, and 5 and Table 1, from Smith and Wang describe the general approach, and contain useful information for anyone designing a contracting cone submerged jet rating facility.

> It is well known that a pair of Helmholtz coils produces a magnetic field of uniform intensity over a core area in the neighborhood of the magnetic axis and in the common median plane. Shaw has shown theoretically that a uniform field intensity at any desired point off the axis can be secured by reducing the Helmholtz separation. It has been calculated and verified experimentally that a pair of circular coils of 30.776 cm. radius and separated a distance of 14.445 cm. produce a field intensity in the median plane which is uniform to within one part in 500 over a core area of radius 13 cm.
>
> It follows from these last studies that a pair of equal vortex rings separated by a distance 14.445/30.776 = 0.46936 radius will give a velocity distribution over a core area of 13/30.776 = 0.42241 radius, in the median plane between the rings, which will likewise be uniform to within one part in 500. One only needs to build a boundary that follows the shape of one of the stream surfaces inside the core to obtain contracting cones whose velocity distribution over the throat section is uniform within the same precision.

Before the design of a venturi tube or a wind tunnel having uniform throat speeds is discussed, the principle according to which different flows can be pieced together may be mentioned. Consider Fig. 3, where tubes in (a) and (b) give the same velocity distributions across the sections C-C and C'-C'. Then from boundary value considerations it is evident that there will be the same velocity distribution at section C''-C'' if we let the portion of tube A at the left side of C-C be connected to the portion of tube B' at the right side of section C'-C'.

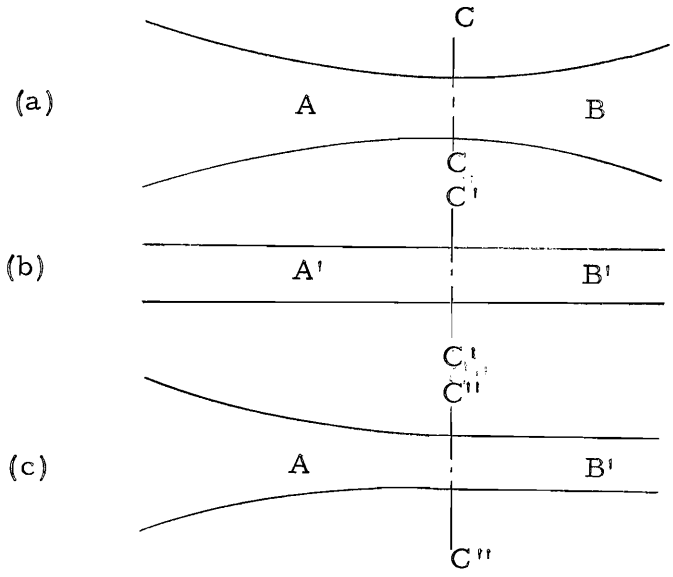

Fig. 3. Possible boundary conditions.

These principles can be utilized in the design of a venturi tube or a wind tunnel in the following way: Let the contracting cone follow one of the inner stream surfaces produced by the two ring vortices up to the median plane. Let it be joined there by a straight tube which, in the case of a wind tunnel, will be the test section. Finally, let there follow a divergent cone of some convenient design. It would seem at first that the divergent cone should also follow another appropriate stream surface chosen from the same family. However, to escape separation everywhere a cone of this type would generally have to be much longer than space limitations would permit. Therefore, in practice the usual straight line diffuser cone is preferable. The combination is shown in Fig. 4.

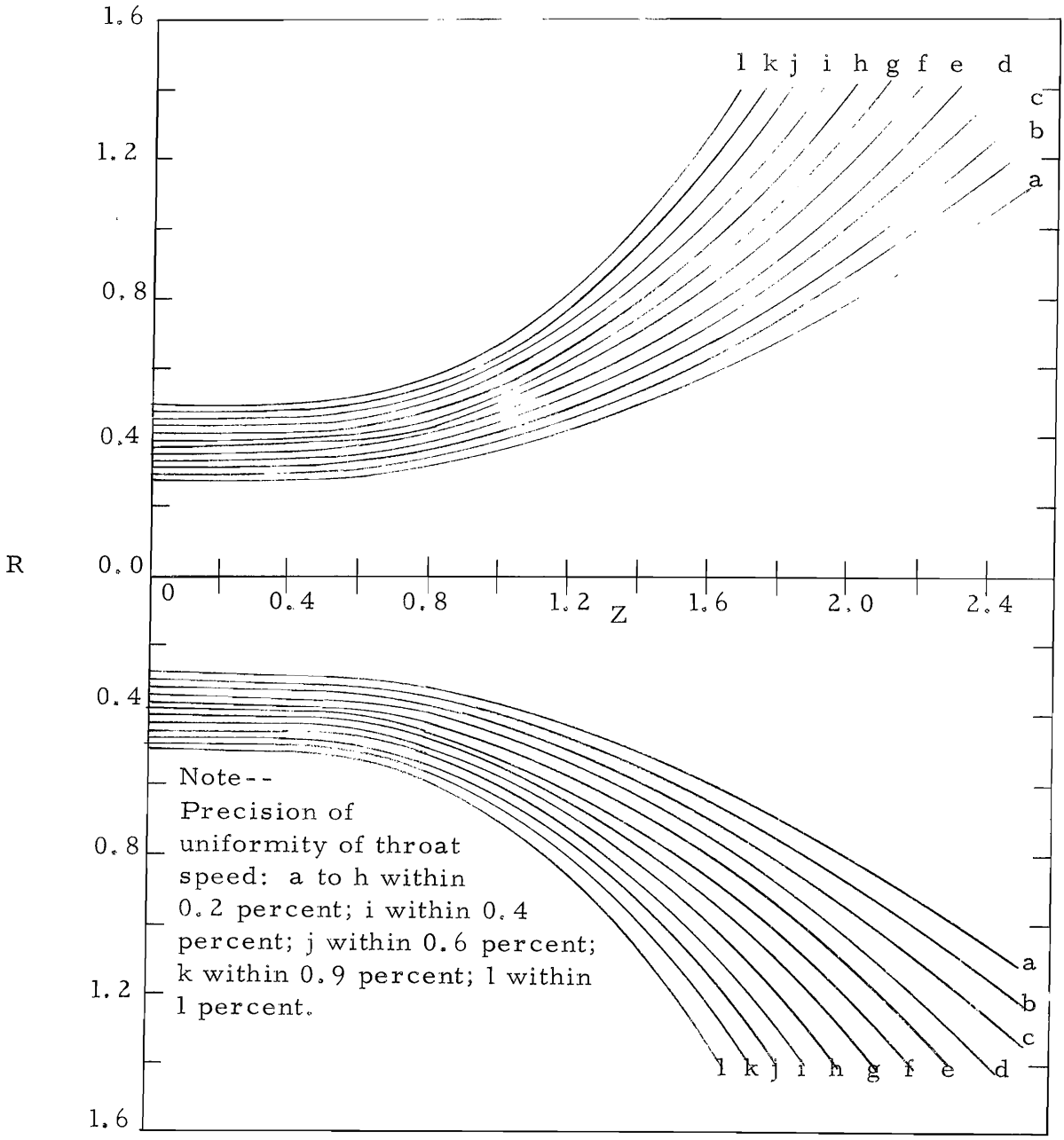

Fig. 5. Boundary forms for contracting cones.

solution by this approach represents an extension to axisymmetric problems of the methods used by several investigators (Stanitz, 1953; Cassidy, 1965; Markland, 1965; and Jeppson, 1966) in solving two-dimensional plane flow problems.

Formulation

To formulate the problems in the $\phi\psi$ plane, equations are needed for r and z as functions of ϕ and ψ. These equations can be obtained from the steady state incompressible equation of continuity and the irrotationality condition (Vallentine, 1959), by following rules of implicit function theory for transformation of variables (Taylor, 1955). The details of this procedure are explained by Jeppson (1966). The resulting equations are

$$\frac{\partial z}{\partial \psi} = -\frac{1}{r}\frac{\partial r}{\partial \phi} \quad . \quad . \quad . \quad . \quad . \quad . \quad . \quad . \quad . \quad . \quad . \quad (1)$$

and

$$\frac{\partial r}{\partial \psi} = \frac{1}{r}\frac{\partial z}{\partial \phi} \quad . \quad . \quad . \quad . \quad . \quad . \quad . \quad . \quad . \quad . \quad . \quad (2)$$

An equation exclusively in r as a function of ϕ and ψ can be obtained by differentiating Eq. 1 with respect to ϕ and Eq. 2 with respect to ψ, combining the results to eliminate $\partial^2 z/\partial\psi\partial\phi$, and finally substituting for $\partial z/\partial\phi$ from Eq. 2.

region. The axisymmetrical problem of a free jet issuing from a convergent nozzle can be formulated in one-half of any plane containing the axis of symmetry. This portion has been transformed to the $\phi\psi$ plane and the boundary value problem for $r(\phi, \psi)$ formulated in the lower portion of Fig. 6. The boundary conditions are obtained as follows:

1. Incoming section. Several possible conditions might be used for the boundary condition through the entering jet upstream from the convergent nozzle, depending upon the nature of the problem for which the nozzle is to be designed. If the incoming fluid is uniform with a velocity, V_o, the condition is

$$\partial r/\partial \phi = 0 \qquad \text{or} \qquad r = \sqrt{\frac{\psi}{\pi V_o}}$$

Either condition will give identical results. The formulation in Fig. 6 suggests that a nonuniform velocity distribution can be obtained by letting the condition for this boundary be given by $r = f(\psi)$ which describes the desired velocity distribution. The computer program permits any desired velocity distribution to be specified, even though such a specification may violate the irrotationality condition. The assumption involved in obtaining solutions for nonuniform incoming velocity distributions needs additional investigation.

2. Conduit wall upstream from nozzle. The condition for the conduit upstream from the nozzle is $r = r_p$, where r_p is the constant radius of the conduit.

3. Convergent nozzle. The convergence of the nozzle can be specified in a number of ways. For a design problem in which a prescribed velocity distribution is to exist along the wall of the nozzle, the third condition shown of Fig. 1 applies, namely

$$\left(\frac{\partial r}{\partial \phi}\right)^2 + r^2 \left(\frac{\partial r}{\partial \psi}\right)^2 = \frac{1}{[V^2(\phi)]} \qquad (7)$$

This condition is obtained from relations (Jeppson, 1966) between the inverse functions $r(\phi, \psi)$ and $V(\phi, \psi)$.

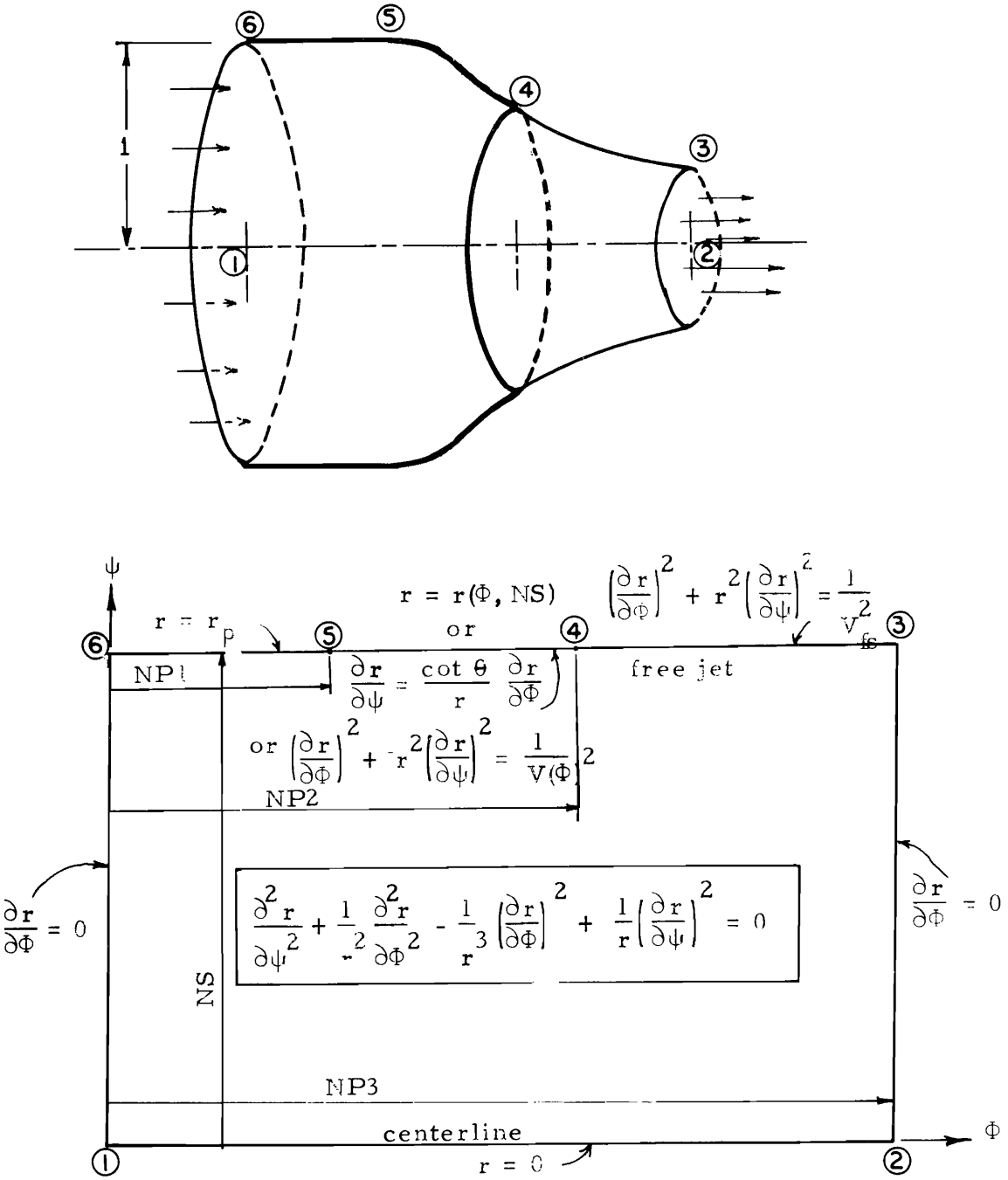

Figure 6. Formulation of the boundary value problem for the function $r(\phi,\psi)$ for a free jet issuing from a converging nozzle.

The convergence of the nozzle might also result by specifying local angles. In this case, the boundary condition is

$$\frac{\partial r}{\partial \psi} = \frac{\cot \theta}{r} \frac{\partial r}{\partial \phi} \quad . \quad . \quad . \quad . \quad . \quad . \quad . \quad . \quad . \quad . \quad . \quad . \quad (8)$$

where θ is the local angle given discretely or as a function of ϕ. Eq. 8 is obtained from the inverse relation between $r(\phi, \psi)$ and $\theta(\phi, \psi)$.

Finally local values of the radius might be specified giving the condition that

$$r = r(\phi, NS) \quad . \quad . \quad . \quad . \quad . \quad . \quad . \quad . \quad . \quad . \quad . \quad . \quad (9)$$

where NS represents the number of the grid line coinciding with the final stream function.

4. Free jet. The boundary condition for the free jet is obtained by noting that axial symmetry requires the gravitational force to be negligible. As a result of this assumption, the velocity is constant and the condition

$$\left(\frac{\partial r}{\partial \phi}\right)^2 + r^2 \left(\frac{\partial r}{\partial \psi}\right)^2 = \frac{1}{V_{fs}^2} \quad . \quad . \quad . \quad . \quad . \quad . \quad . \quad . \quad . \quad (10)$$

results from relations between $r(\phi, \psi)$ and $V(\phi, \psi)$. The magnitude of V_{fs} must be determined at the tip of the nozzle. For the boundary condition of the nozzle given by Eq. 7, the velocity V_{fs} must equal the velocity $V(\phi)$ specified at the end of the nozzle. When either of the other boundary conditions for the nozzle are specified, V_{fs} must be solved for from $r(\phi, \psi)$ to satisfy relationships between $r(\phi, \psi)$ and $V(\phi, \psi)$.

5. Test section of jet. For a uniform velocity at the test section of the jet, the boundary condition is

$$\frac{\partial r}{\partial \phi} = 0 \quad . \quad . \quad . \quad . \quad . \quad . \quad . \quad . \quad . \quad . \quad . \quad . \quad . \quad (11)$$

6. Centerline. The boundary condition for the centerline is

$$r = 0 \quad . \quad . \quad . \quad . \quad . \quad . \quad . \quad . \quad . \quad . \quad . \quad . \quad . \quad . \quad (12)$$

The procedures which have been followed to obtain the finite difference solution falls in the category of methods using an inner as well as the usual outer iteration. The inner iteration is necessary in order to satisfy the finite difference operators at each grid point, since they consist of fourth degree polynomials. This implicit nature of the operators result because of the nonlinearity in the differential Eq. 3. Only for linear differential equations are the finite differences operators explicit in terms of the value of the function at the grid points in question. The inner iteration has been accomplished by the Newton-Raphson method (Kunz, 1957). The outer iteration uses the Gauss-Siedel method of successive displacements with an overrelaxation factor (Forsythe and Wasow, 1960). By this method, the field of grid points is repeatedly swept across in a manner consistent with the so-called "property A" (see Forsythe and Wasow, 1960) until the change between consecutive iterations is less than some prescribed error parameter. At each point, the value is adjusted to satisfy the equation.

$$r(I, J) = r(I, J) - \omega\left[\overline{r}(I, J) - r(I, J)\right] \quad . \quad . \quad . \quad . \quad . \quad . \quad (19)$$

where ω is the overrelaxation factor and $\overline{r}(I, J)$ is the value of the variable which satisfies the finite difference operator. The most recently computed values from surrounding grid points are used in all computations involving them.

Nature of solution

It is not feasible to give more than a sample of a solution obtained by the methods described earlier. Fig. 7 is a plot of the r and z coordinates obtained by specifying the local angles condition along the nozzle boundary. In addition to the coordinates of the flow net, a complete solution also gives the direction and magnitude of the velocity of the flow at each of these grid points. This latter information is obtained directly from $r(\phi,\psi)$ and $z(\phi,\psi)$ by using difference approximation for derivates relating the several inverse functions (Jeppson, 1966). Furthermore, as indicated earlier, considerable flexibility exists in specifying the problem. In addition to the capability of specifying the velocity (or pressure) distribution along the wall of the nozzle, it is possible to specify any incoming velocity distribution. This latter specification may consist of an algebraic expression for the velocity distribution or discrete values for it, such as might be obtained from laboratory measurements. If the normal derivative condition is specified along the test section boundary, the shape of the nozzle will always be that necessary to establish a uniform velocity distribution at this section of the jet. Since in real fluids boundary layers form adjacent to surfaces in which the viscous effects are strong, some deviation in practice is expected from the predicted results.

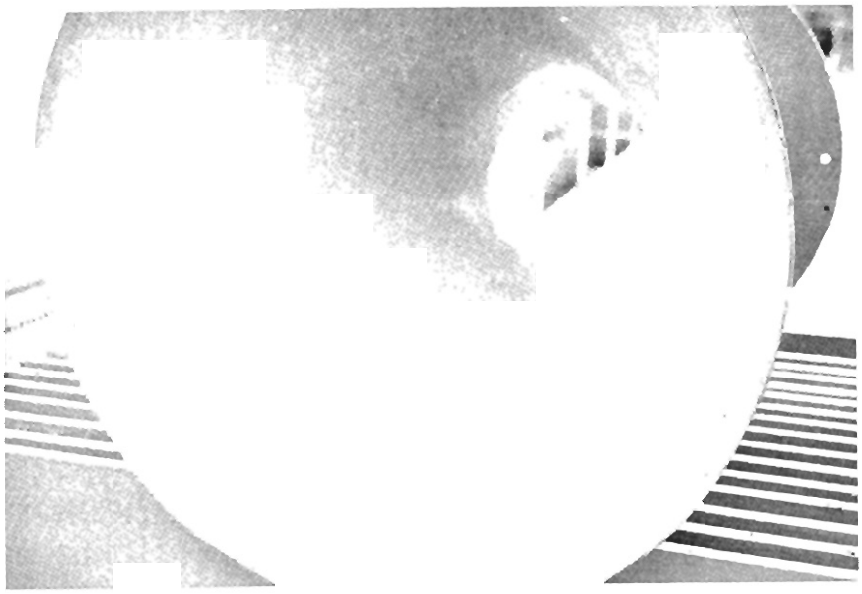

Fig. 9. Model 8-inch contracting cone (d)

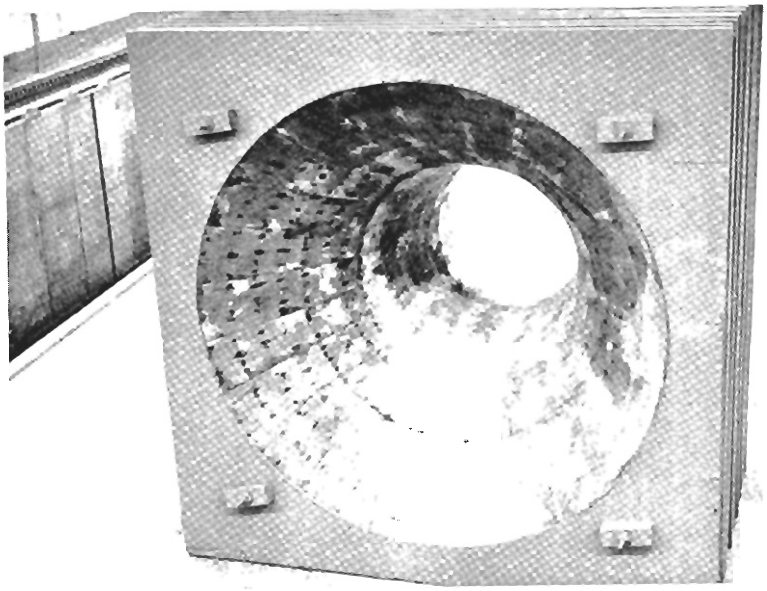

Fig. 10. Model 16-inch contracting cone (e)

Fig. 11. Model 16-inch contracting cone (e) combined with the 8-inch converging nozzle

perhaps be of sufficient cross-sectional area for rating current meters. At this stage of the research project, it was contemplated that a 24-inch nozzle or cone would be required for rating the standard current meter used by the USGS.

Experimental Facilities

The hydraulic testing of the model cones and nozzle was conducted in the Fluid Mechanics Laboratory which is located in the Engineering and Physical Science Building. A flume recessed in the floor having a width of 5 feet and a depth of 5 feet was employed. Water was pumped (using one or more pumps) from a tank located in the basement of the laboratory into a 12-inch diameter pipeline which discharges into the flume. The depth of flow in the flume was controlled by a tailgate located near the downstream end of the flume. The water surface elevations upstream and downstream from the cones or nozzle (Fig. 12) were measured in stilling wells using hook gages which were read to the closest thousandth-of-a-foot (0.001 foot). The flow rate was determined by discharging the water into a weighing tank and measuring with a stop watch the length of time required to accumulate a particular weight of water. Each flow rate measurement was converted to a mean jet velocity using the cross-sectional area of the nozzle or cone throat. After obtaining a flow rate measurement, the water was discharged into the sump (tank), where it was recirculated through the system.

Velocities in the flow field were measured with a pitot tube having an outside diameter of 1/8 inch. The pitot tube was connected by two plastic tubes to a manometer mounted on the flume wall. The water levels in the manometer were read by eye using a mirror. The location of the pitot tube in the flow field is described in the x, y, and z planes as shown in Figs. 12 and 13. The origin of the coordinate system is the intersection of the axis and outlet of the nozzle or cone. The positive direction for x is measured downstream from the nozzle or cone outlet. A negative x distance would then be upstream from the nozzle or cone outlet (inside the nozzle or cone). The pitot tube is located in the plane perpendicular to the flow direction by y and z coordinates. The location of point velocity measurements in the horizontal plane, y, and vertical plane, z, are shown in the Fig. 13. The distance between points 1 and 2, 2 and 3, 8 and 9, and 9 and 10 is 1/16 of the outlet diameter, whereas the distance between the remaining points is 1/8 the outlet diameter. The adjustable carriage used for placing the pitot tube at a specified point in the flow field is shown in Figs. 14 and 15.

The rotation speed of the current meter cups was obtained by either using an earphone and stop watch or recording each revolution with time on an Oscilloriter recording system (Fig. 16). The earphone and stop watch could only be used with the Pygmy current meter for low velocities. In most cases the recording system was used.

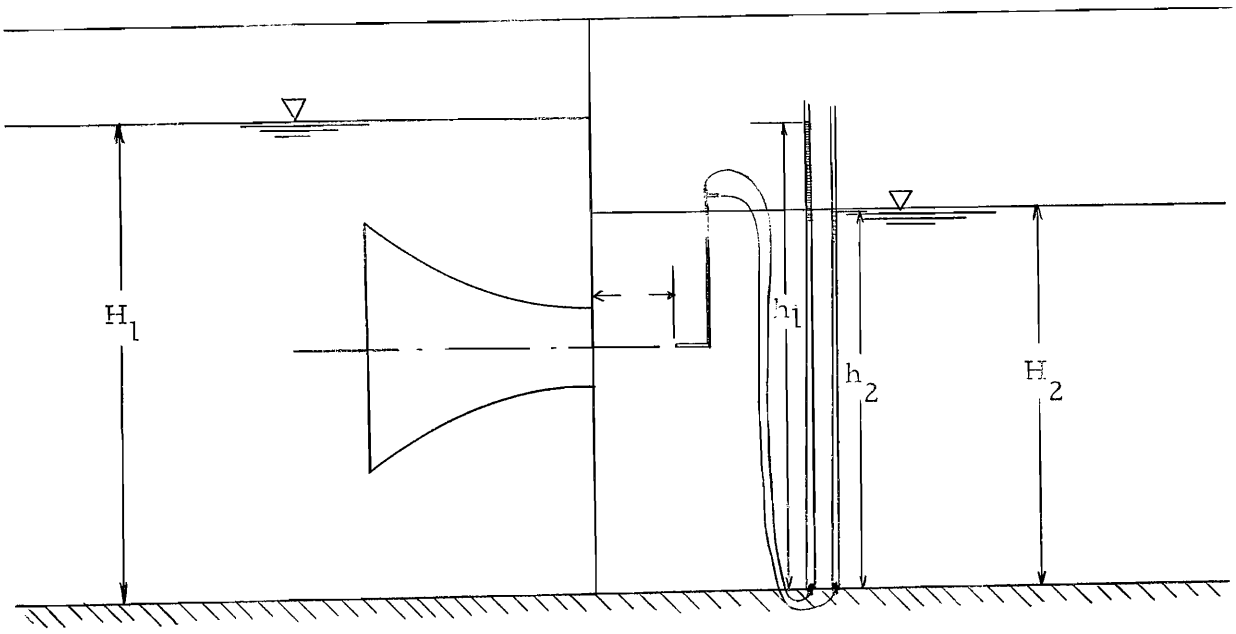

(a) Definition sketch for 8-inch contracting cone (d).

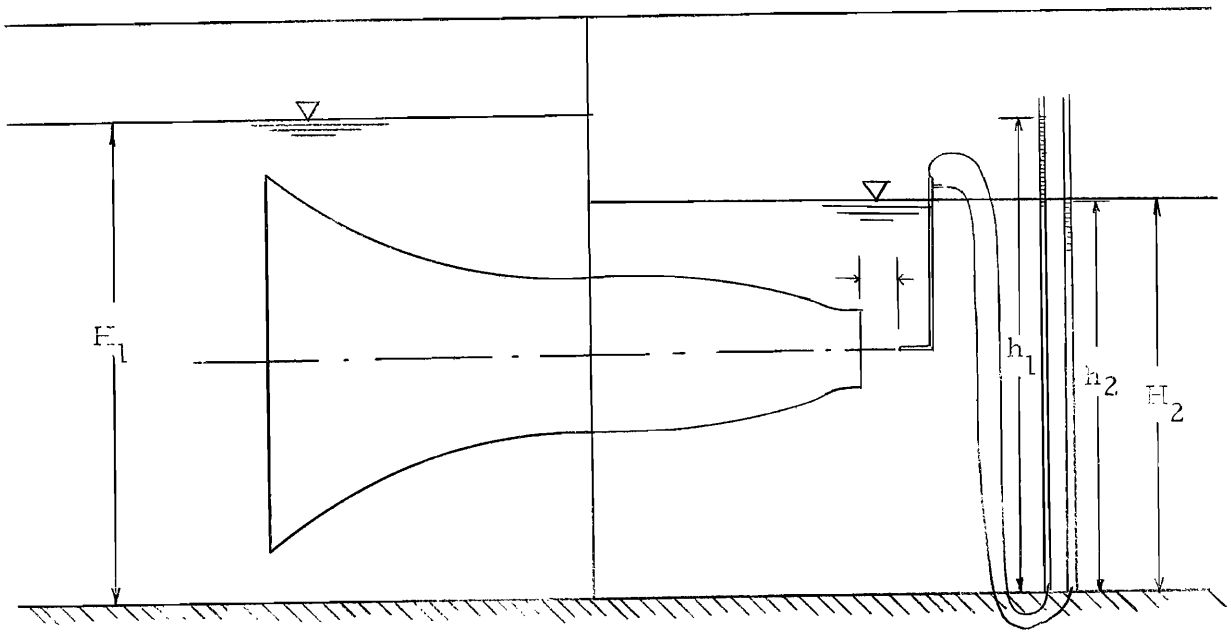

(b) Definition sketch for 8-inch converging nozzle.

Fig. 12. Definition sketch of measurement system for preliminary studies.

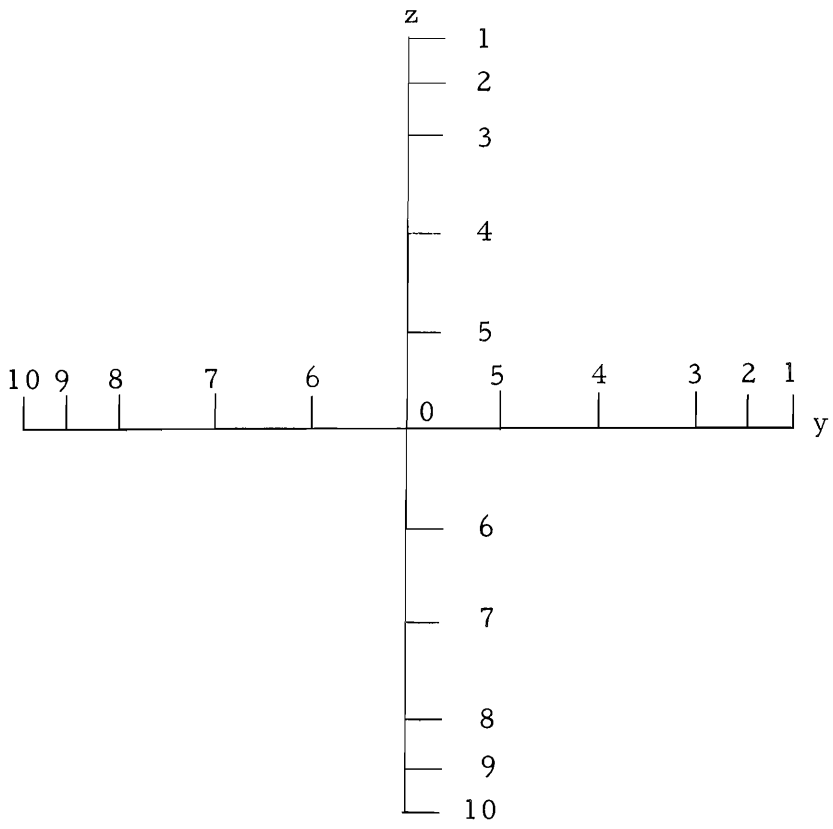

Fig. 13. Location of point velocity measurements in the y-z plane used in preliminary studies.

A better manometer would increase the precision of measurements in this range of velocities.

Conclusions

The hydraulic testing of the model cones showed that a submerged jet having a uniform velocity distribution over a fairly wide range of discharge could be produced using a converging nozzle or contracting cone. The rating of a Pygmy current meter in a submerged jet was accomplished with the error ranging between 1 and 2 percent. Most of the points with the Pygmy current meter were accurate within 1 percent when the 8-inch contracting cone (d) was used. The error ranged between 1 and 3 percent when a Type AA Price current meter was tested in conjunction with a 16-inch contracting cone (e). Based upon these results, a prototype submerged jet contracting cone rating facility could be constructed using a 16-inch outlet diameter.

PROTOTYPE STUDIES

Prototype System

The layout of the prototype system is shown in Fig. 24. The system consists of a head tank 8 feet wide, 10 feet high, and 30 feet long along with a tailwater tank 24 feet long, 6 feet high, and its width varies from 4 feet at the entrance to 3 feet wide for the last 15 feet of tank length. A 16-inch contracting cone (d) was fabricated and placed between the two tanks. The basic components of this system are shown in Figs. 25, 26, and 27.

The prototype system was constructed in the Utah Water Research Laboratory. The water supply for the laboratory is conveyed by means of a 48-inch pipeline from a small reservoir located on the Logan River. Branches from the main pipeline are located throughout the laboratory. The head tank is fed by a 14-inch pipeline, with the discharge being controlled by a 14-inch gate valve.

Once the flow enters the head tank, it must rise and pass over a weir plate whose crest is 8 1/2 feet above the floor. The weir plate was set high enough that free flow will always occur over the weir. Thus, any flow depth changes near the entrance of the cone will not affect the discharge over the weir, thereby allowing a constant discharge to be maintained for the system. The weir plate also serves the dual purpose of reducing the turbulence

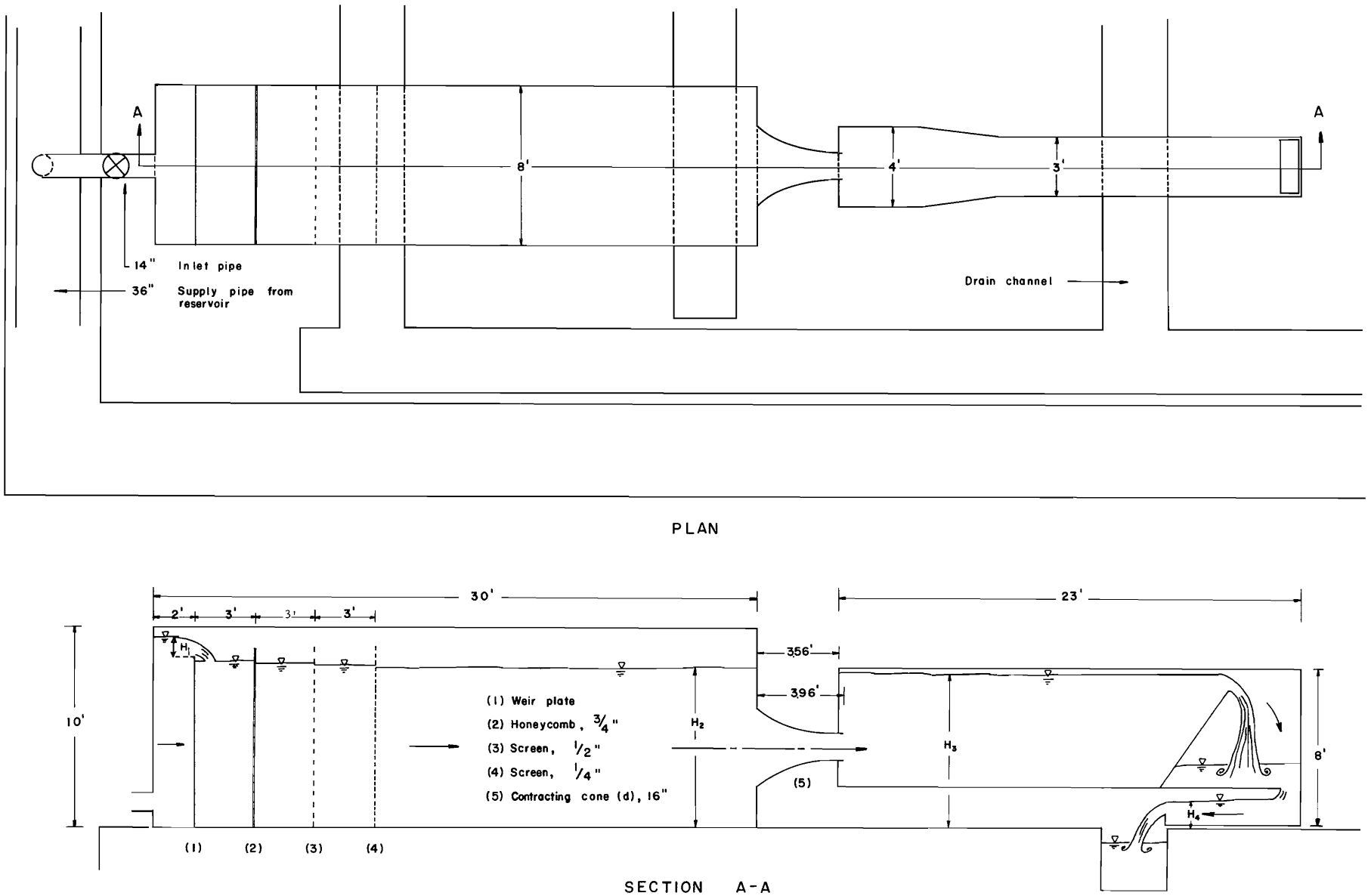

Fig. 24. Layout of prototype system.

Fig. 25. Prototype system showing head tank 16-inch contracting cone (d), and tailwater tank

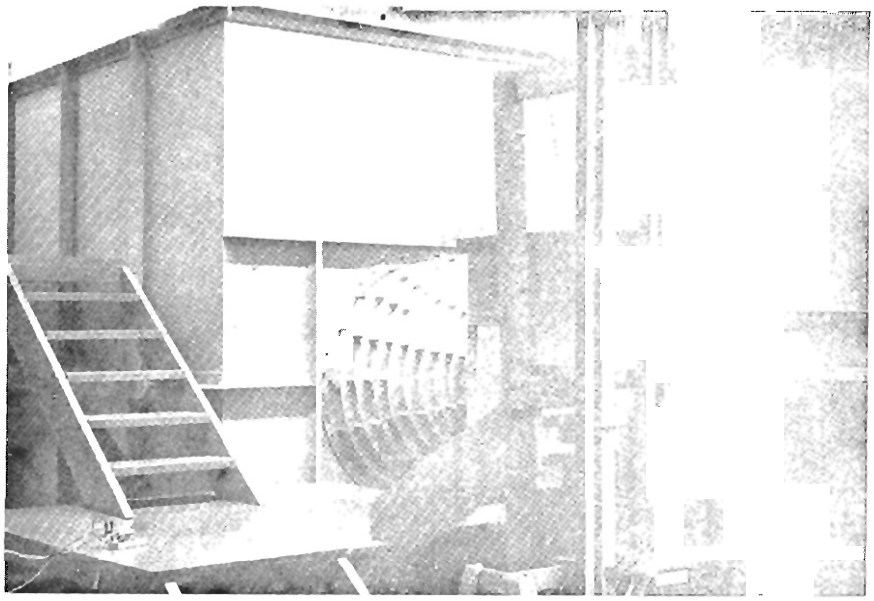

Fig. 26. Instrumentation area for prototype system

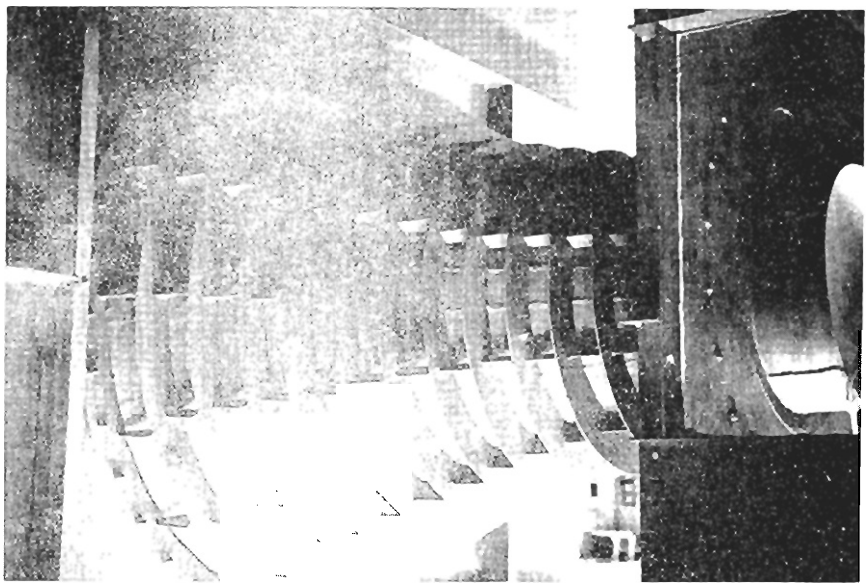

Fig. 27. Prototype 16-inch contracting cone (d) with outlet shown through plexiglass

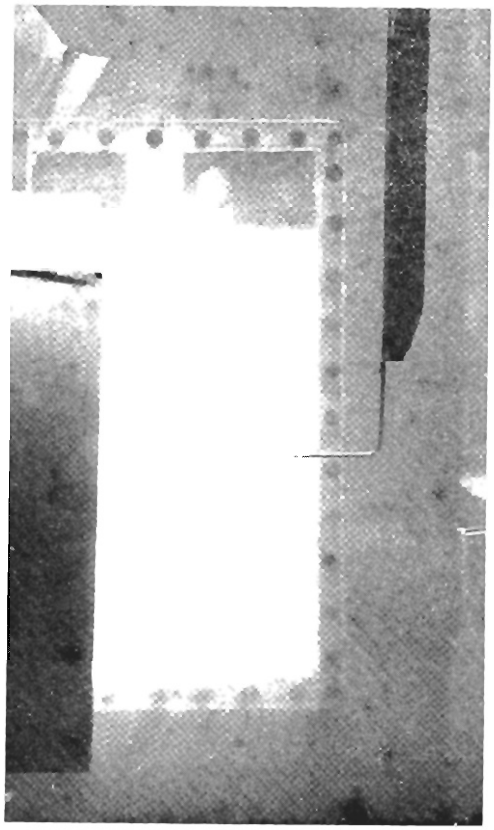

Fig. 36. Pitot tube located at x = 6" in submerged jet

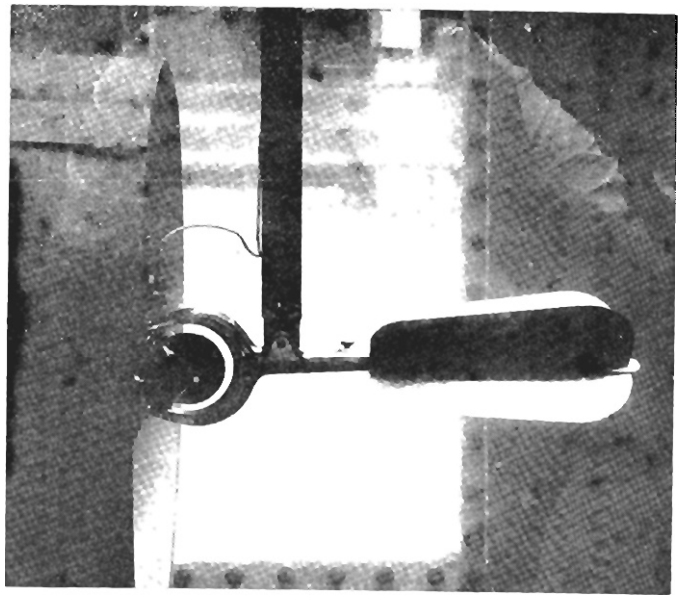

Fig. 37. Current meter located at x = 0" in submerged jet

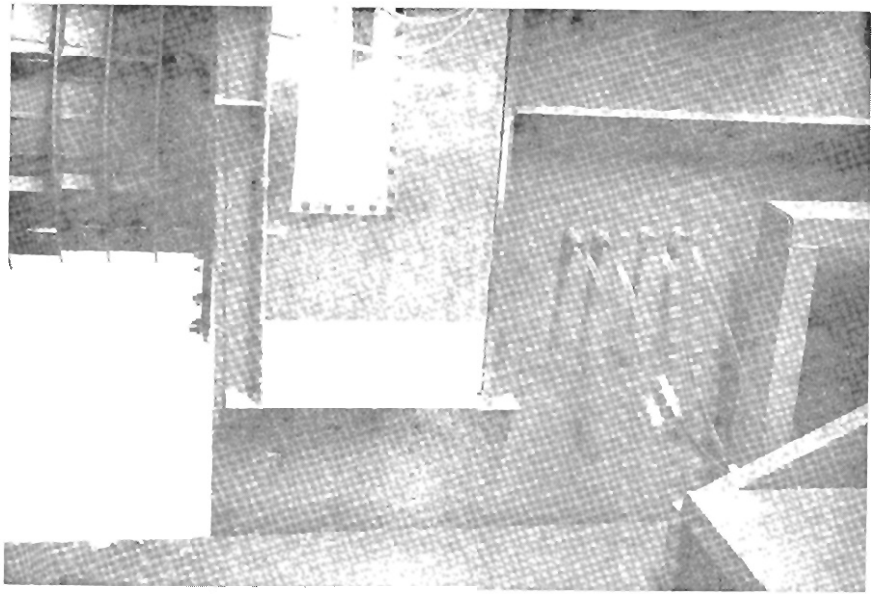

Fig. 38. Outlet of prototype contracting cone with tubing from pitot tube to manometers

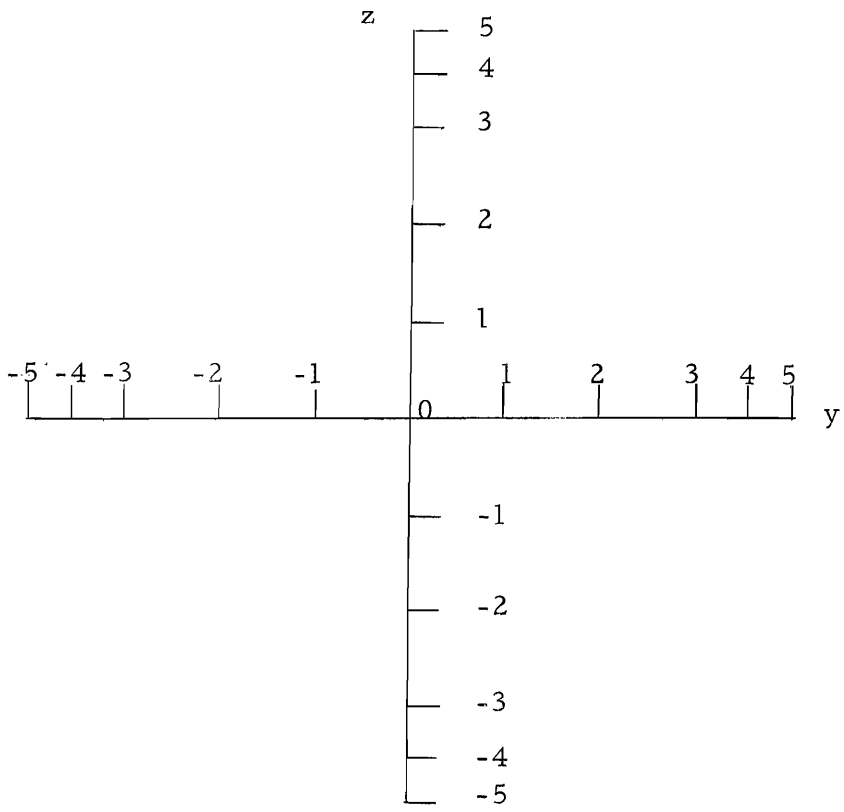

Fig. 39. Location of point velocity measurements in the y-z plane used for prototype studies.

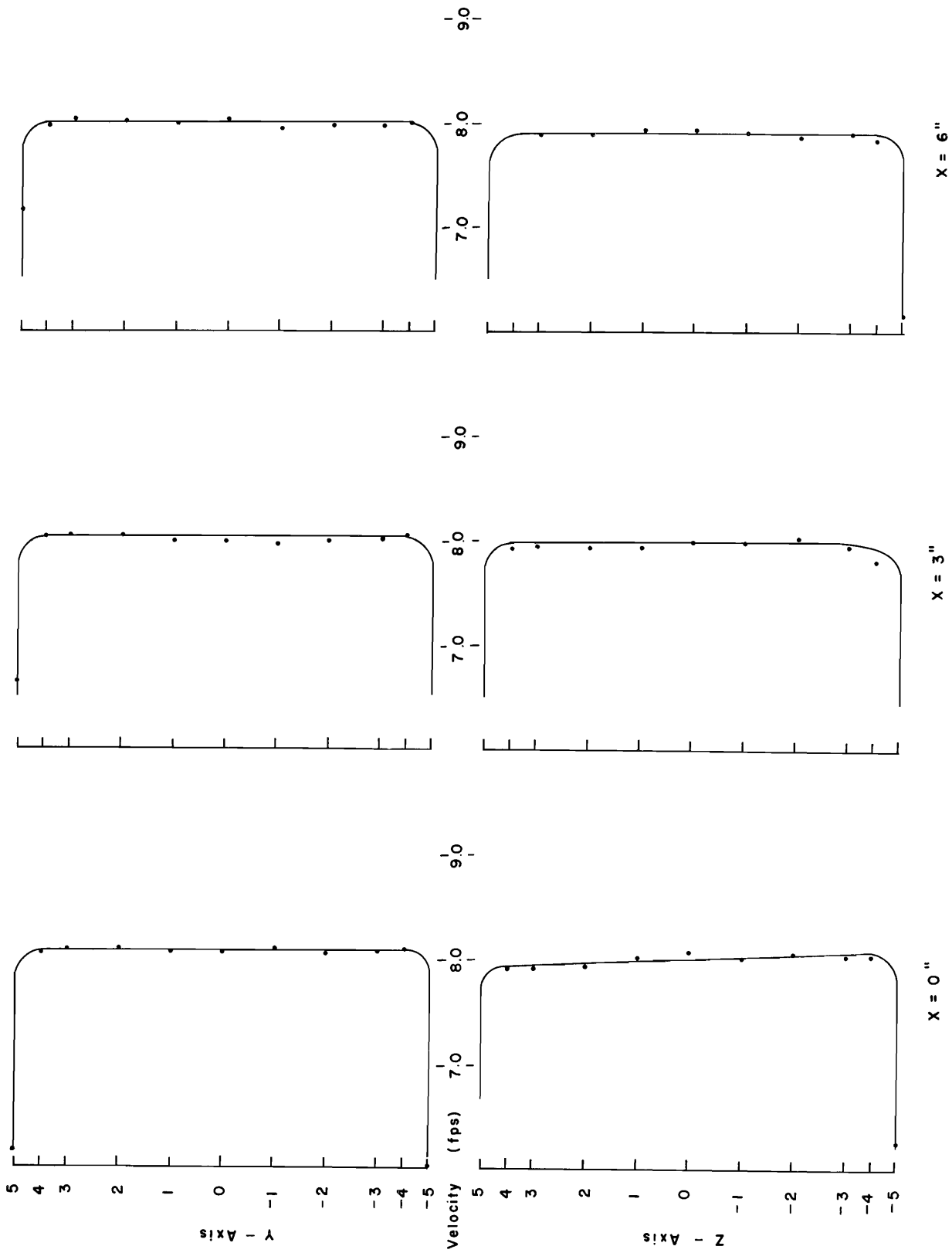

Fig. 48. Velocity distribution of submerged jet from 16-inch contracting cone (d), (V approx. 8 fps). . . . . .

Two Type AA Price current meters, no. 261388 and no. 261392, were available for comparing the towing tank rating equations with the core velocities measured in the submerged jet. The core velocity is computed as the average of point velocity measurements collected at y_2, $-y_2$, z_2, $-z_2$, and z_0y_0. The core area represents 1/4 of the cross-sectional area of the jet. The data acquired under this phase of the research program is given in Table 29. Also, the data has been summarized and presented in Table 3 to allow a comparison of the core velocities with the current meter velocities. The current meter velocities are computed from the towing tank rating equations using the measurements of the current meter cup speed (in revolutions per second) collected in the submerged jet. The data represented in Table 3 has also been plotted in Figs. 49 and 50 in the conventional manner used for current meter ratings. The accuracy attained for velocities less than 1 fps was very satisfying because of the difficulty in making the pitot tube measurements. The single disappointing measurement was the velocity of 8.26 fps recorded for current meter no. 216388.

Table 3. Summary of current meter data.

Core Velocity, fps	Velocity from Current Meter No. 216388, fps	Velocity from Current Meter No. 216392, fps
0.29	0.25	0.31
0.42	0.43	0.45
0.67	0.67	0.68
1.25	1.25	1.24
1.47	1.46	1.48
2.36	2.31	2.35
3.81	3.71	3.87
5.27	5.20	5.35
6.16	6.14	6.16
8.55	8.26	8.50

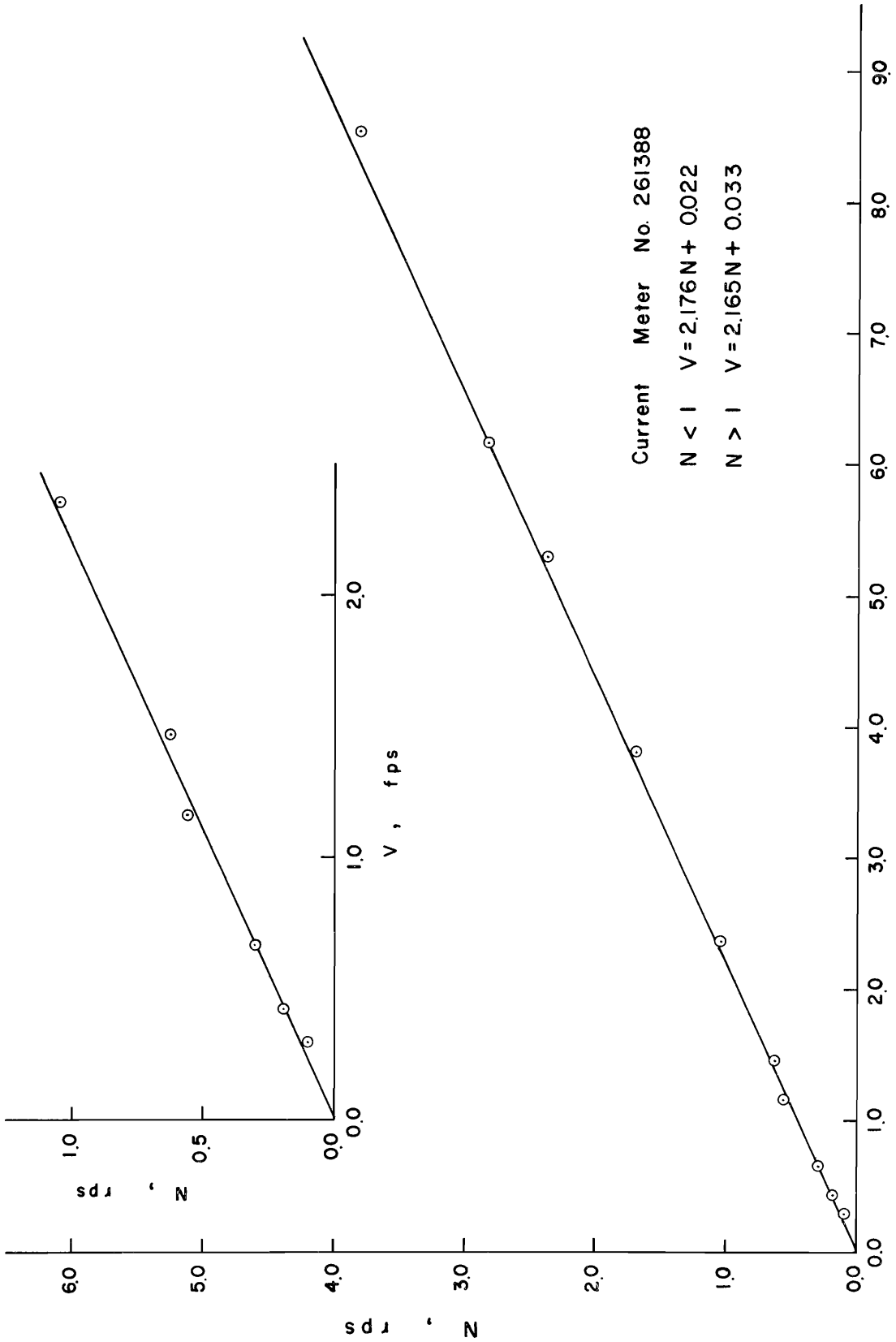

Fig. 49. Comparison of prototype core velocities with rating for current meter 261388 . . . . . .

Table 4. 8" Contracting Cone (d), free jet.

Point Loc.	x = 1.5" $V^2/2g$ inches	x = 1.5" V fps.	x = 0" $V^2/2g$ inches	x = 0" V fps.	x = 3" $V^2/2g$ inches	x = 3" V fps.
y_1	25.70	11.74	24.10	11.37	25.75	11.76
y_2	29.20	12.52	27.70	12.19	30.50	12.79
y_3	29.45	12.57	27.40	12.13	30.14	12.72
y_4	28.90	12.45	26.90	12.02	29.70	12.63
y_5	28.55	12.38	26.85	12.00	29.42	12.57
y_0	28.45	12.36	26.45	11.91	29.45	12.57
y_6	28.55	12.45	26.80	11.99	29.48	12.58
y_7	28.48	12.36	26.91	12.02	29.70	12.63
y_8	28.85	12.44	27.20	12.08	30.10	12.71
y_9	29.00	12.48	27.55	12.16	30.40	12.77
y_{10}	26.80	11.99	26.20	11.86	25.80	11.77
z_1	23.40	11.21	18.80	10.04	23.20	11.16
z_2	25.50	11.70	24.65	11.50	26.95	12.03
z_3	25.70	11.74	25.20	11.63	27.65	12.18
z_4	26.20	11.86	25.96	11.80	28.20	12.30
z_5	26.70	11.97	26.60	11.95	28.77	12.43
z_0	27.80	12.21	27.35	12.12	29.72	12.63
z_6	28.70	12.41	28.60	12.39	30.70	12.84
z_7	30.10	12.71	29.25	12.53	31.50	13.00
z_8	30.60	12.81	30.40	12.77	32.80	13.27
z_9	30.20	12.73	30.80	12.86	33.35	13.38
z_{10}	27.10	12.06	27.30	12.10	26.90	12.02
	Q cfs.	V_m fps.	Q cfs.	V_m fps.	Q cfs.	V_m fps.
y	4.31	12.24	4.21	11.96	4.38	12.44
z	4.26	12.10	4.29	12.19	4.41	12.53
	H_1 feet	H_2 feet	H_1 feet	H_2 feet	H_1 feet	H_2 feet
y	4.292		4.292		4.486	
z	4.292		4.333		4.503	

Table 9. Converging Nozzle, submerged jet (V approx. 4 fps).

Point Loc.	x = 0" $V^2/2g$ inches	x = 0" V fps.	x = 3" $V^2/2g$ inches	x = 3" V fps.	x = 6" $V^2/2g$ inches	x = 6" V fps.
y_4	3.10	4.08	3.12	4.09	3.10	4.08
y_0	3.10	4.08	3.12	4.09	3.10	4.08
y_7	3.10	4.08	3.12	4.09	3.10	4.08
z_4	3.10	4.08	3.13	4.10	3.20	4.14
z_0	3.10	4.08	3.13	4.10	3.10	4.08
z_7	3.10	4.08	3.10	4.08	3.10	4.08
	Q cfs.	V_m fps.	Q cfs.	V_m fps.	Q cfs.	V_m fps.
*	1.40	4.01	1.39	3.99	1.40	4.01
+	1.40	4.01	1.39	3.99	1.40	4.01
:	1.40	4.01			1.39	3.99
	H_1 feet	H_2 feet	H_1 feet	H_2 feet	H_1 feet	H_2 feet
*	3.913	3.614	3.912	3.613	3.911	3.618
+	3.916	3.614	3.910	3.616	3.913	3.617
:	3.929	3.613			3.913	3.615

Pygmy Current Meter

	$N_{ave.}$ rps.	$V_{ave.}$ fps.	$N_{ave.}$ rps.	$V_{ave.}$ fps.	$N_{ave.}$ rps.	$V_{ave.}$ fps.
y_0z_0	4.26	4.16	4.29	4.19	4.28	4.19

* Unobstructed jet
\+ Pitot tube in jet
: Pygmy meter in jet

Table 10. Converging Nozzle, submerged jet (V approx. 2 fps).

Point Loc.	x = 0" $V^2/2g$ inches	x = 0" V fps.	x = 3" $V^2/2g$ inches	x = 3" V fps.	x = 6" $V^2/2g$ inches	x = 6" V fps.
y_4	0.77	2.03	0.79	2.06	0.80	2.07
y_0	0.77	2.03	0.79	2.06	0.79	2.06
y_7	0.77	2.03	0.79	2.06	0.80	2.07
z_4	0.77	2.03	0.79	2.06	0.80	2.07
z_0	0.77	2.03	0.79	2.06	0.80	2.07
z_7	0.77	2.03	0.79	2.06	0.80	2.07
	Q cfs.	V_m fps.	Q cfs.	V_m fps.	Q cfs.	V_m fps.
*	0.70	2.00	0.69	1.99	0.69	1.99
+	0.69	1.99	0.70	2.00	0.70	2.00
:	0.69	1.99	0.70	2.00	0.70	2.00
	H_1 feet	H_2 feet	H_1 feet	H_2 feet	H_1 feet	H_2 feet
*	3.660	3.562	3.659	3.562	3.659	3.562
+			3.659	3.562	3.659	3.562
:	3.664	3.562	3.659	3.562	3.659	3.563
	Pygmy Current Meter					
	$N_{ave.}$ rps.	$V_{ave.}$ fps.	$N_{ave.}$ rps.	$V_{ave.}$ fps.	$N_{ave.}$ rps.	$V_{ave.}$ fps.
y_0z_0	2.01	2.01	2.11	2.11	2.10	2.10

* Unobstructed jet
\+ Pitot tube in jet
: Pygmy meter in jet

Table 17. 8" Contracting Cone (d), submerged jet (V approx. 11.5 fps).

Point Loc.	$V^2/2g$ inches	V fps.	$V^2/2g$ inches	V fps.	$V^2/2g$ inches	V fps.
y_4	24.90	11.56	24.70	11.51	24.60	11.49
y_0	24.90	11.56	24.80	11.54	24.52	11.47
y_7	24.90	11.56	24.70	11.51	24.60	11.49
z_4	24.90	11.56	24.80	11.54	24.52	11.47
z_0	24.90	11.56	24.80	11.54	24.52	11.47
z_7	24.90	11.56	24.70	11.51	24.45	11.45
	Q cfs.	V_m fps.	Q cfs.	V_m fps.	Q cfs.	V_m fps.
*	3.75	10.65	3.73	10.59	3.73	10.59
+	3.75	10.65	3.75	10.65	3.71	10.53
:	3.68	10.56	3.72	10.56	3.71	10.53
	H_1 feet	H_2 feet	H_1 feet	H_2 feet	H_1 feet	H_2 feet
*	4.583	2.466	4.573	2.437	4.557	2.446
+	4.598	2.469	4.583	2.457	4.572	2.458
:	4.638	2.429	4.583	2.451	4.568	2.443
	Pygmy Current Meter					
	$N_{ave.}$ rps.	$V_{ave.}$ fps.	$N_{ave.}$ rps.	$V_{ave.}$ fps.	$N_{ave.}$ rps.	$V_{ave.}$ fps.
y_0z_0	11.86	11.42	11.88	11.44	11.98	11.53

* Unobstructed jet
\+ Pitot tube in jet
: Pygmy meter in jet

Table 1. 16" Contracting Cone (e), submerged jet (V approx. 1.6 fps).

Point Loc.	x = 0" $V^2/2g$ inches	x = 0" V fps.	x = 3" $V^2/2g$ inches	x = 3" V fps.	x = 6" $V^2/2g$ inches	x = 6" V fps.
y_4	0.51	1.65	0.48	1.61	0.42	1.50
y_0	0.51	1.65	0.48	1.61	0.40	1.47
y_7	0.51	1.65	0.48	1.61	0.42	1.50
z_4	0.51	1.65	0.48	1.61	0.42	1.50
z_0	0.51	1.65	0.48	1.61	0.40	1.47
z_7	0.51	1.65	0.48	1.61	0.42	1.50
	Q cfs.	V_m fps.	Q cfs.	V_m fps.	Q cfs.	V_m fps.
*	2.25	1.61	2.22	1.59	2.21	1.58
+	2.23	1.60	2.21	1.58	2.21	1.58
:	2.23	1.60	2.21	1.58	2.23	1.60
	H_1 feet	H_2 feet	H_1 feet	H_2 feet	H_1 feet	H_2 feet
*	3.661	3.605	3.662	3.605	3.651	3.596
+	3.662	3.605	3.662	3.605	3.652	3.595
:	3.666	3.605	3.663	3.606	3.652	3.595
	Current Meter W-261388					
	$N_{ave.}$ rps.	$V_{ave.}$ fps.	N_{ave} rps.	$V_{ave.}$ fps.	$N_{ave.}$ rps.	$V_{ave.}$ fps.
y_0z_0	0.74	1.63	0.74	1.64	0.70	1.55

* Unobstructed jet
\+ Pitot tube in jet
: Price meter in jet

Table 19. 16" Contracting Cone (e), submerged jet (V approx. 3.3 fps).

Point Loc.	x = 0" $V^2/2g$ inches	x = 0" V fps.	x = 3" $V^2/2g$ inches	x = 3" V fps.	x = 6" $V^2/2g$ inches	x = 6" V fps.
y_4	2.02	3.29	2.00	3.28	2.00	3.28
y_0	2.02	3.29	2.00	3.28	2.00	3.28
y_7	2.02	3.29	2.00	3.28	2.00	3.28
z_4	2.02	3.29	2.00	3.28	2.00	3.28
z_0	2.02	3.29	2.00	3.28	2.00	3.28
z_7	2.02	3.29	2.00	3.28	2.00	3.28
	Q cfs.	V_m fps.	Q cfs.	V_m fps.	Q cfs.	V_m fps.
*	4.66	3.34	4.59	3.29	4.60	3.29
+	4.66	3.34	4.58	3.28	4.58	3.28
:	4.66	3.34	4.66	3.33	4.61	3.30
	H_1 feet	H_2 feet	H_1 feet	H_2 feet	H_1 feet	H_2 feet
*	3.658	3.478	3.658	3.478	3.653	3.473
+	3.659	3.485	3.660	3.482	3.659	3.478
:	3.672	3.482	3.672	3.485	3.665	3.482
	Current Meter W-261388					
	$N_{ave.}$ rps.	$V_{ave.}$ fps.	$N_{ave.}$ rps.	$V_{ave.}$ fps.	$N_{ave.}$ rps.	$V_{ave.}$ fps.
y_0z_0	1.50	3.28	1.50	3.28	1.49	3.26

* Unobstructed jet
\+ Pitot tube in jet
: Price meter in jet

Table 20. 16" Contracting Cone (e), submerged jet (V approx. 0.9 fps).

Point Loc.	x = 0" $V^2/2g$ inches	x = 0" V fps.	x = 3" $V^2/2g$ inches	x = 3" V fps.	x = 6" $V^2/2g$ inches	x = 6" V fps.
y_4	0.15	0.90	0.16	0.93	0.15	0.90
y_0	0.15	0.90	0.16	0.93	0.15	0.90
y_7	0.15	0.90	0.16	0.93	0.15	0.90
z_4	0.15	0.90	0.16	0.93	0.15	0.90
z_0	0.15	0.90	0.16	0.93	0.15	0.90
z_7	0.15	0.90	0.16	0.93	0.15	0.90
	Q cfs.	V_m fps.	Q cfs.	V_m fps.	Q cfs.	V_m fps.
*	1.18	0.85	1.19	0.85	1.18	0.85
+	1.19	0.85	1.18	0.85	1.18	0.85
:	1.19	0.85	1.19	0.85	1.18	0.85
	H_1 feet	H_2 feet	H_1 feet	H_2 feet	H_1 feet	H_2 feet
*	3.660	3.629	3.660	3.628	3.660	3.628
+	3.660	3.628	3.660	3.628	3.660	3.629
:	3.661	3.629	3.660	3.628	3.660	3.629
	Current Meter W-261388					
	$N_{ave.}$ rps.	$V_{ave.}$ fps.	$N_{ave.}$ rps.	$V_{ave.}$ fps.	$N_{ave.}$ rps.	$V_{ave.}$ fps.
y_0z_0	0.39	0.87	0.39	0.87	0.39	0.87

* Unobstructed jet
\+ Pitot tube in jet
: Price meter in jet

Table 26. 16" Contracting Cone (d), submerged jet (V approx. 2.2 fps).

Point Loc.	x = 0"		x = 3"		x = 6"	
	$V^2/2g$ inches	V fps.	$V^2/2g$ inches	V fps.	$V^2/2g$ inches	V fps.
y_5	0.548	1.714	0.458	1.567	0.765	2.026
y_4	0.683	1.914	0.840	2.123	0.870	2.161
y_3	0.690	1.924	0.840	2.123	0.870	2.161
y_2	0.690	1.924	0.840	2.123	0.863	2.152
y_1	0.698	1.935	0.840	2.123	0.863	2.152
y_0	0.690	1.924	0.840	2.123	0.863	2.152
$-y_1$	0.698	1.935	0.840	2.123	0.863	2.152
$-y_2$	0.698	1.935	0.840	2.123	0.863	2.152
$-y_3$	0.690	1.924	0.840	2.123	0.863	2.152
$-y_4$	0.683	1.914	0.840	2.123	0.870	2.161
$-y_5$	0.465	1.580	0.420	1.501	0.375	1.419
z_5	0.465	1.580	0.330	1.331	0.285	1.284
z_4	0.600	1.794	0.825	2.104	0.825	2.104
z_3	0.630	1.839	0.855	2.142	0.758	2.016
z_2	0.713	1.955	0.855	2.142	0.863	2.152
z_1	0.713	1.955	0.855	2.142	0.863	2.152
z_0	0.675	1.903	0.840	2.123	0.863	2.152
$-z_1$	0.690	1.924	0.870	2.161	0.863	2.152
$-z_2$	0.690	1.924	0.870	2.161	0.863	2.152
$-z_3$	0.698	1.935	0.863	2.152	0.863	2.152
$-z_4$	0.698	1.935	0.863	2.152	0.863	2.152
$-z_5$	0.563	1.738	0.608	1.806	0.750	2.006

Table 27. 16" Contracting Cone (d), submerged jet (V approx. 4.5 fps).

Point Loc.	x = 0" $V^2/2g$ inches	x = 0" V fps.	x = 3" $V^2/2g$ inches	x = 3" V fps.	x = 6" $V^2/2g$ inches	x = 6" V fps.
y_5	2.36	3.56	2.46	3.63	3.00	4.01
y_4	3.32	4.22	4.46	4.89	4.35	4.83
y_3	3.32	4.22	4.42	4.87	4.26	4.78
y_2	3.32	4.22	4.42	4.87	4.26	4.78
y_1	3.30	4.21	4.45	4.89	4.26	4.78
y_0	3.32	4.22	4.42	4.87	4.26	4.78
$-y_1$	3.35	4.24	4.42	4.87	4.24	4.77
$-y_2$	3.38	4.26	4.42	4.87	4.24	4.77
$-y_3$	3.43	4.29	4.42	4.87	4.24	4.77
$-y_4$	3.38	4.26	4.42	4.87	4.22	4.76
$-y_5$	1.94	3.23	2.63	3.75	2.87	3.93
z_5	1.95	3.24	1.27	2.61	0.60	1.79
z_4	3.23	4.16	4.11	4.70	3.32	4.22
z_3	3.26	4.19	4.25	4.77	3.99	4.63
z_2	3.26	4.19	4.32	4.82	4.05	4.66
z_1	3.26	4.19	4.42	4.87	4.18	4.73
z_0	3.26	4.19	4.48	4.91	4.16	4.72
$-z_1$	3.38	4.26	4.50	4.91	4.20	4.75
$-z_2$	3.45	4.30	4.59	4.96	4.20	4.75
$-z_3$	3.45	4.30	4.59	4.96	4.20	4.75
$-z_4$	3.41	4.28	4.56	4.96	4.20	4.75
$-z_5$	2.20	3.43	3.66	4.05	2.70	3.81